16th World Conference on Earthquake, 16WCEE 2017
Santiago Chile, January 9th to 13th 2017
Paper N° 1760
Registration Code: S-V1462908614

EXPERIMENTAL DYNAMIC BEHAVIOUR OF HISTORICAL BUILDINGS: THE PALAZZO MARCHESALE IN S. GIULIANO DI PUGLIA, ITALY

G. Bongiovanni[(1)],G. Buffarini[(1)], P. Clemente[(1)], F. Saitta[(1)],
A. De Sortis[(2)], M. Nicoletti[(2)], G. Rossi[(3)], F. Scafati[(4)]

[(1)]*ENEA Casaccia, giovanni.bongiovanni@enea.it, giacomo.buffarini@enea.it, paolo.clemente@enea.it, fernando.saitta@enea.it*
[(2)]*Civil Protection Dept., PCM, Adriano.DeSortis@protezionecivile.it, Mario.Nicoletti@protezionecivile.it*
[(3)]*Office for the reconstruction of San Giuliano di Puglia, g.rossi@mailpw.it*
[(4)]*ENEA Casaccia, Visiting Engineer, f.scafati@alice.it*

Abstract

Identification of dynamic characteristics of historical buildings is an important step that is necessary for two basic reasons: to assess possible dynamic behavior of such complex structures during strong events and to gain experience on the dynamic behavior of historical buildings such that the experience and database can be used in future design and analyses. Actually, data on dynamic behavior of complex structures such as historical buildings are scarce. The databases are in general obtained from dynamic testing of structures (forced vibration, ambient vibration, etc), and from analyses of data from instrumented structures. With this purpose, ENEA, in accordance with the Italian Civil Protection Department and the Municipality of San Giuliano di Puglia organized a research project for seismic monitoring of relevant structures in the framework of the reconstruction of San Giuliano di Puglia, Italy. Among the monitored buildings there is the Palazzo Marchesale, an old masonry structure hosting the new City Hall. Some low-intensity seismic events have been recorded up to now, which allowed analyzing the seismic behavior under events of different magnitude and distance from the site. The experimental results have compared with those of a numerical analysis.

Keywords: Masonry structures, Seismic analysis, Experimental dynamics.

1 Introduction

Palazzo Marchesale (Fig. 1), located in the historical center of San Giuliano di Puglia, is an arrangement of four masonry buildings seriously damaged by the 2002 earthquake. The buildings are characterized by irregular stone masonry texture, with no definite mortar planes. Seismic improving interventions were done after the quake. These consisted in mortar injections in masonry, substitution of some floors with new ones having laminated wood structure, and retrofit of vaulted roofs by means of FRP. Furthermore, the Palace was divided into buildings of regular shape (T, A, B and C), with seismic separation joints to ensure independent movement of some parts, obtained simply by operating vertical cuts in the masonry. The effectiveness of the joints depends upon the wideness and cleaning of the gap obtained during works. Therefore, the tower T at the entrance of the courtyard is linked to building C but structurally separated from A and B. These latest, where the city halls is placed, are structurally independent. In the framework of a research project for the monitoring of some relevant structures in San Giuliano di Puglia, the ancient palace was chosen as relevant case study and a permanent accelerometric array was installed.

As test of the permanent one and for the dynamic characterization of the structure, a temporary seismometer array was used to record ambient vibrations. Resonance frequencies, modal shapes and damping were identified. On the basis of the experimental results, a Finite Element Model (FEM) was defined and updated [1]. Nonlinear elements capable of cracking [2] were used and a first seismic analysis was performed. Recently, some low intensity earthquakes hit the area and data were acquired by the permanent monitoring system. The analyses of the data are summarized in this paper, giving a critical comparison with the ambient vibration results. The experimental dynamic results were also compared with those of a linear FEM.

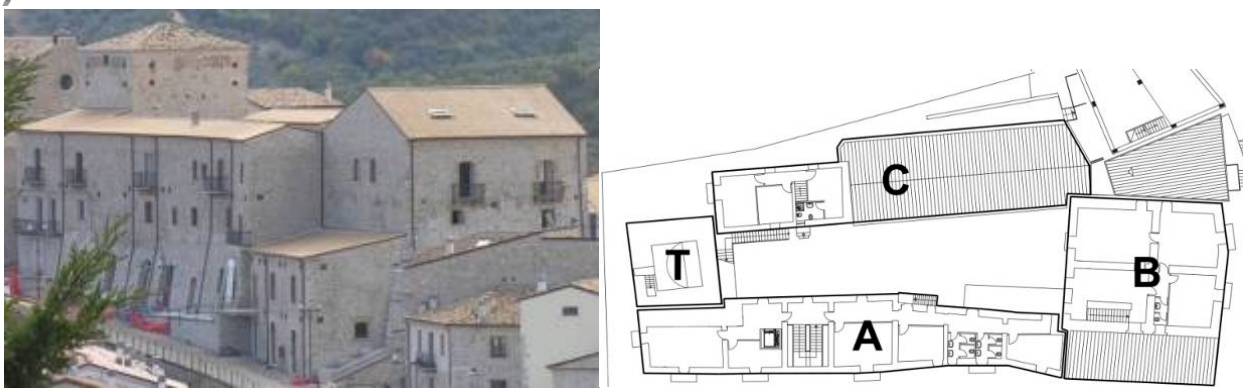

Fig. 1 – The *Palazzo Marchesale*: view (left) and general plan (right).

2 Dynamic characterization and finite element modelling

Several finite element models have been set up in order to explain as well as possible the experimental behavior. In details blocks T+C, A and B have been firstly considered as structurally separated, according to the design choices. The configuration in which block A is connected with T+C or with B have been also analyzed. Finally the model in which all the blocks are connected has been studied. The latter gave results very close to the experimental one, obtained under ambient vibration and was used also for a preliminary interpretation of the recorded seismic behavior. In Table 1 the resonance frequencies obtained with this last model are reported.

Table 1 – Resonance frequencies.

Ambient vibrations		**FEM model**	
***f* (Hz)**	**Type**	***f* (Hz)**	**Descr.**
5.7	$T_y + A_{y,T}$	5.5	$T_y + A_{y,T}$
6.3	$B_y + A_{y,B}$	6.5	$B_y + A_{y,B}$
6.7	T_x	6.8	T_x
8.3	$A_{y,m}$	7.3	$A_{y,m}$
8.5	B_x	8.1	B_x
9.8	A_x	9.8	A_x

$\mathbf{T_y}$ = Tower prevalent motion along Y
$\mathbf{T_x}$ = Tower prevalent motion along X
$\mathbf{B_y}$ = Building B prevalent motion along Y
$\mathbf{B_x}$ = Building B prevalent motion along X
$\mathbf{A_x}$ = Building A prevalent motion along X
$\mathbf{A_y}$ = Building A prevalent motion along Y
$\mathbf{A_{y,T}}$ = Building A along Y direction, with maximum amplitude near T
$\mathbf{A_{y,B}}$ = Building A along Y direction, with maximum amplitude near B
$\mathbf{A_{y,m}}$ = Building A along Y direction, with maximum amplitude at midpoint
$\mathbf{A_{t,s}}$ = Symmetric Torsion of Building A
$\mathbf{A_{t,as}}$ = Asymmetric Torsion of Building A

The comparison with the experimental values obtained by ambient vibration [1] shows the best match when the whole palace with an elastic modulus of the material $E=2.3\cdot10^9 N/m^2$ is considered. The modal shape components at the position of the sensors are represented in Fig. 2. The ineffectiveness of the seismic joints can be explained by the low level of vibration and will be discussed in a future research.

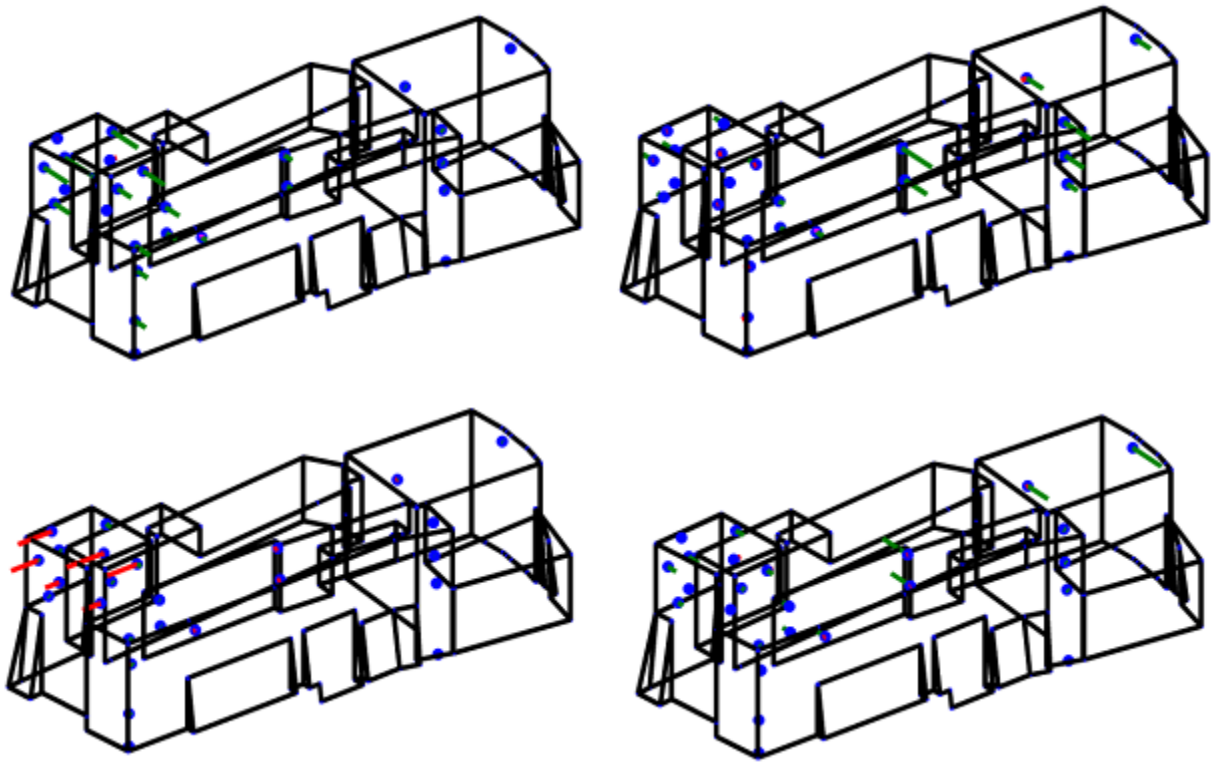

Fig. 2 – FEM modal shape components at sensor location.

3 Accelerometer monitoring system

Since 2012 the palace is equipped with a long-term monitoring system. The system belongs to the Italian national network for the monitoring of the seismic response of buildings, bridges and dams of public property, the Seismic Observatory of Structures (OSS) of the Italian National Civil Protection Dept. of the Presidency of the Council of Ministers [5].

For the seismic monitoring the following buildings have been considered: building A, developed from level -1 to level 1; a little room on level -2 is present in the left corner (Fig. 3); building B, which includes levels 0 and 1 but also levels -1and -2 in some parts; the tower T, which starts from level 0 and presents levels 1, 2 and 3 and is structurally connected to building C.

The accelerometric network (Fig. 3) is composed by 26 sensors. 4 of them are triaxial, 8 are biaxial and 14 are uniaxial accelerometers, so the total number of channel is 42. In building A three sensors (A1) were deployed on the floor and two sensors (A4) under the ceiling at level -1. Three other sensors (A9) were put on level 0 as well as two sensors respectively on the floor (A6) and under the ceiling (A7). On level 1, five accelerometers are on the floor and six under the ceiling. This deployment should be able to record both longitudinal and transversal movements of building A, in which one side is much higher than the other.

In building B three accelerometers (A2) were put on level -1, three (A10) on level 0 and three (A16 and A17) on level 1. The latest should be able to analyze both the translational and torsional modes of building B. The tower was instrumented by means of four accelerometers (A21, A22, A23 and A24) on level 2, four on the floor of level 3 (A8 and A19) and four under the ceiling of level 3 (A24, A25, A26 and A27).

Another triaxial accelerometer is in the courtyard, about 10 m below the ground level. This sensor belongs to the RAN strong motion accelerometric network [6] and should be able to record the seismic input to the building.

A comparison of modal identification with data acquired by temporary seismometers was reported in a previous study [1].

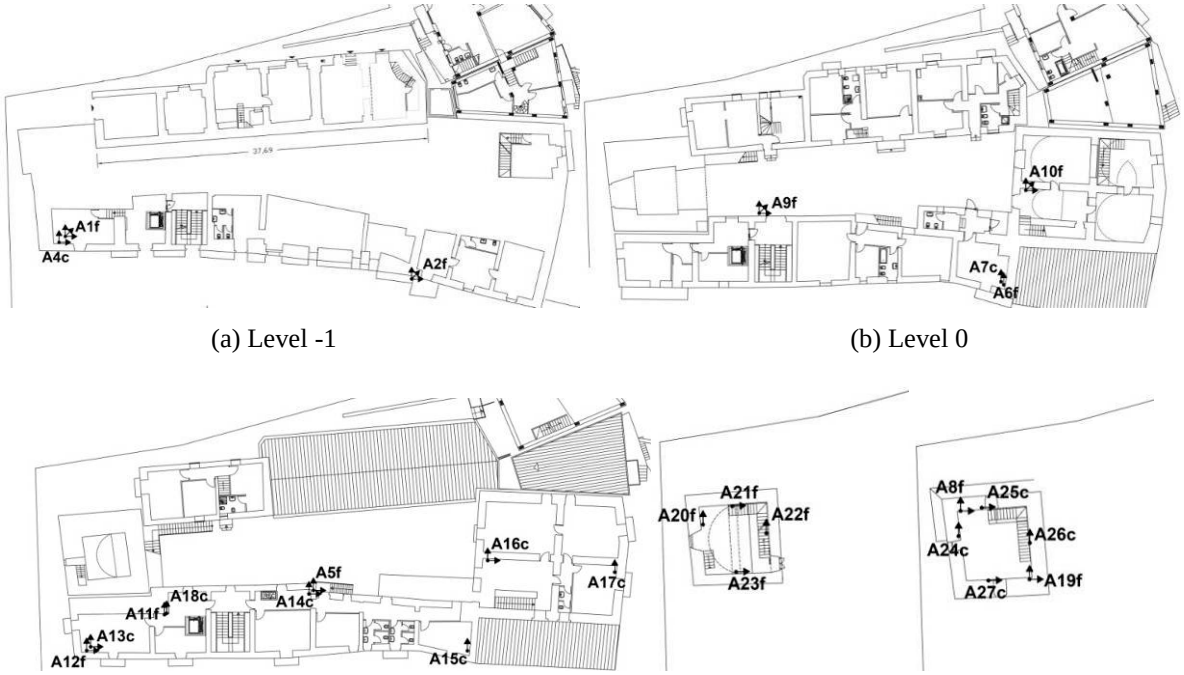

(a) Level -1 (b) Level 0

(c) Level 1 (d) Level 2 (Tower) (e) Level 3 (Tower)

Fig. 3 – Accelerometric network (f=floor, c=ceiling; x direction = left-right direction).

4 Recorded earthquakes at the site

On December 20th, 2013, a first relevant earthquake was recorded by the sensors placed on the building (13:08:58 UTC, M_w=4.2, M_l=3.8, Lat. 41.677 N and Lon. 14.283 E). The Peak Ground Accelerations (PGA) in the three NS, WE and UP directions, respectively, recorded at the site by RAN are reported in Table 2. Also the components with reference to the main axes of the building are shown in order to allow a comparison with those recorded on the basement of the building. The time histories are shown in Fig. 4. In Table 3, the intensity I_A measured according the Arias formula are reported.

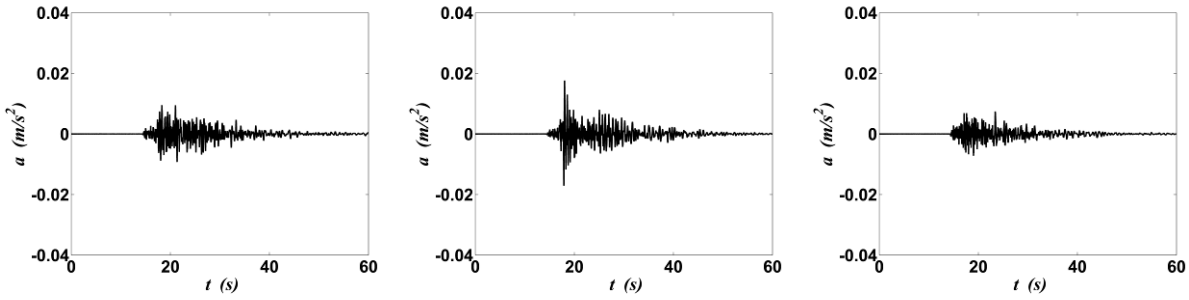

Fig. 4 – Time histories recorded at the site by RAN during the 2013 earthquake: NS (left), WE (middle) and UP (right) components.

Through standard Fourier analysis the frequency content of each time history was obtained and represented in Fig. 5. The largest values of the spectral amplitude are in the frequency range 0-5 Hz, whereas the first mode of the structure is close to 6 Hz. Anyway, some energy is contained in the range 5-10 Hz, which is that of major interest for the structure under study.

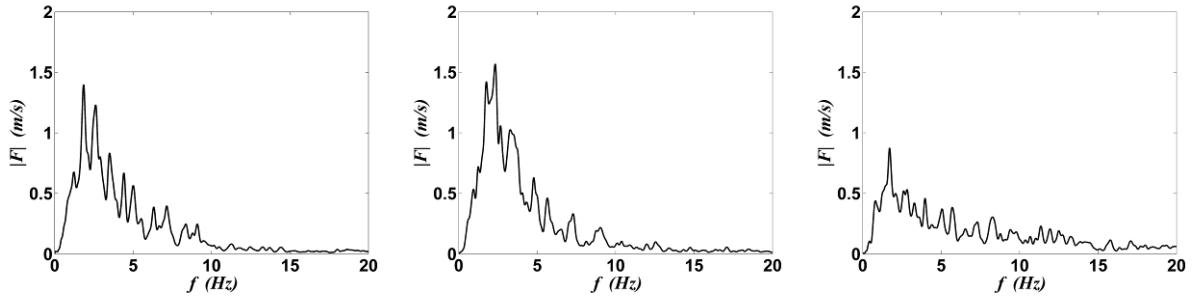

Fig. 5– Fourier amplitude spectra of the 2013 earthquake: NS (left), WE (middle) and UP (right) components.

Another relevant earthquake was detected on December 24th, 2014 (11:40:10 UTC, M_w=4.3, M_l=4.1, Lat. 41.698 N and Lon. 14.957 E, depth 17.6). The time histories recorded by RAN are plotted in Fig. 6. The Fourier spectra (Fig. 7) show a wider band of higher amplitudes with respect to the 2013 event, especially the harmonic components in the 0-10 Hz range.

The I_A reveals the larger energy related with this latter event. In tables 2 and 3 the data recorded at the base of the structure (sensors A1 and A2) are also given.

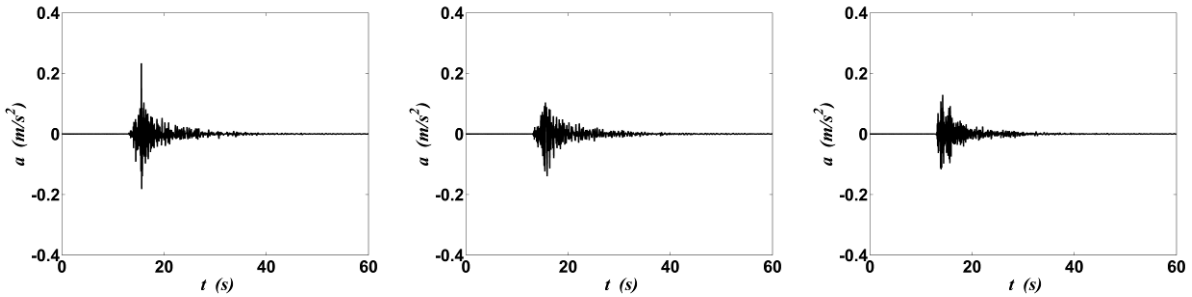

Fig. 6 – Time histories in the 2014 earthquake: NS (left), WE (middle) and UP (right) components.

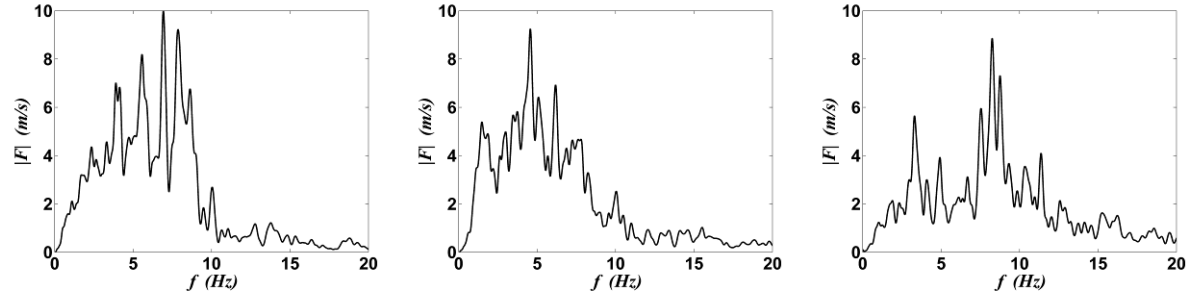

Fig. 7– Fourier amplitude spectra of the 2014 earthquake: NS (left), WE (middle) and UP (right) components.

Table 2 – Seismic events: magnitude and PGA.

Date	M_l	M_w	PGA (cm/s^2)											
			Soil (RAN)			Soil (RAN)			Structure - A1			Structure - A2		
			WE	NS	Z	X	Y	Z	X	Y	Z	X	Y	Z
12-20-2013 13:08:58	3.8	4.2	0.9	1.8	0.7	1.8	1.1	0.7	2.4	1.8	1.3	2.5	1.4	1.3
12-24-2014 11:40:10	4.1	4.3	23.3	14.0	12.9	15.8	23.2	12.9	22.4	30.4	20.6	20.5	43.0	24.5

Table 3 – Arias intensity for recordings on soil and on the structure (level -1).

Date	I_A (cm/s)		
	Soil (RAN)	Structure	
		A1	A2
12-20-2013	6.91E-03	1.16E-04	1.09E-04
12-24-2014	4.58E-01	1.04E-02	1.30E-02

5 Experimental seismic behavior

During the two seismic events, data were acquired by the 42 channels with a sampling ratio of 250 samples/s. Recordings lasting about 60 s were acquired during the two earthquakes. Data were analyzed in the frequency domain in order to determine auto and cross power spectral density functions [3]. It is worth reminding that, at resonance frequencies, the coherence function computed for two simultaneously recorded output signals has values close to one and phase angle close to zero or to ±180 degrees. The Welch periodogram method has been used for this analysis. In order to minimize leakage a Hanning time window function was used. Every signal has been divided into 4 time windows, with 50% of windows overlapping.

For the two events, Fig. 8 shows the auto spectral density, normalized with respect to the maximum, of some sensors placed on the tower (T), whereas phase factor and coherence function are shown in Fig. 9. The peak at 5 Hz for sensors in y direction is the most evident. Sensors in x direction show more than one peak, with maximum amplitude at about 6.1 Hz.

Sensors placed on building B highlight the presence of the y-direction prevalent motion of that building at about 5.7 Hz (Figs. 10 and 11). Finally, the mode with prevalent motion of the intermediate part of block A is revealed by the spectra of Fig. 12 at 7.4 Hz.

The spectra related to the 2014 earthquake are represented by red lines in the Figures. The most important aspect is the significant shift in frequency of the modal shapes. Table 4 resumes the frequencies extracted in the two earthquakes and the comparison with that observed for ambient vibration analysis. The differences between the resonance frequencies under ambient vibrations and that during the 2013 and 2014 seismic events can be due to the nonlinear behavior of the masonry under different vibration levels and a different effectiveness of the seismic joints (Fig. 13). In both cases the onset of damage can be excluded; indeed, the maximum interstorey drift resulted 0.3/1000, far from the expected damage threshold.

The modal shapes were easily extracted by comparing the cross spectra and confirmed by the direct extraction using the Frequency Domain Method (FDD) [4]. A representation of the first four modes on a schematic plot of the building is given in Fig. 14 for those extracted in the 2013 earthquake and Fig. 15 for those of the 2014 event.

Figure 16 shows the Modal Assurance Criterion (MAC) [7] value for the first mode shape, the maximum being at frequency correspondent to that of the first experimental mode in the two earthquakes. To be clear, the Figures represent the MAC between the first analytical mode and the first singular vector evaluated at each frequency step.

Table 4 – Experimental frequencies (Hz)

Earthquake 12.20.2013 $f^{(2013)}$	**Earthquake 12.24.2014** $f^{(2014)}$	**Ambient vibration** $f^{(a)}$	**Modal shape**	$\frac{\left\|f^{(2013)} - f^{(a)}\right\|}{f^{(a)}}$	$\frac{\left\|f^{(2014)} - f^{(a)}\right\|}{f^{(a)}}$
5.0	4.2	5.7	$T_y + A_{y,T}$	12.2	26.3
5.7	4.8	6.3	$B_y + A_{y,B}$	9.5	23.8
6.1	5.2	6.7	T_x	8.9	22.4
7.2	6.6	8.3	$A_{y,m}$	13.2	20.5
7.4	7.2	8.5	B_x	12.9	15.3

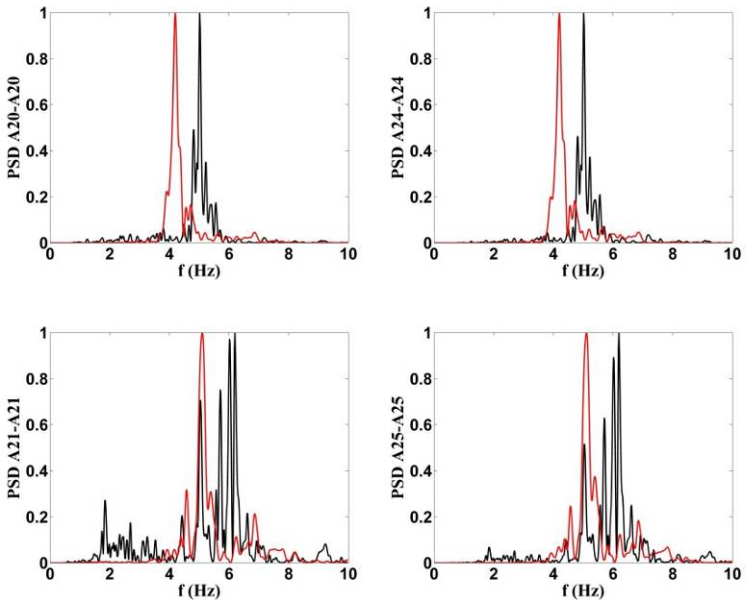

Fig. 8– Normalized auto spectral density in the 2013 (black) and 2014 (red) earthquakes: tower T.

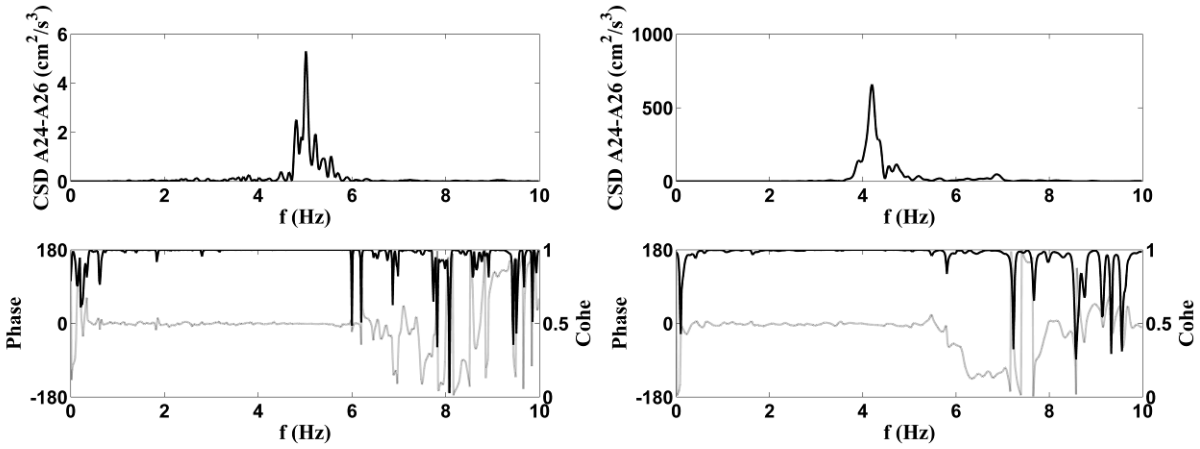

Fig. 9 – Cross spectral density for some sensor in the 2013 earthquake: tower T.

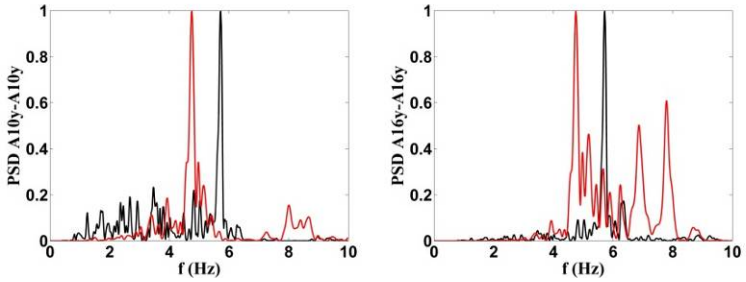

Fig. 10 – Normalized auto spectral density in the 2013 (black) and 2014 (red) earthquakes: building B.

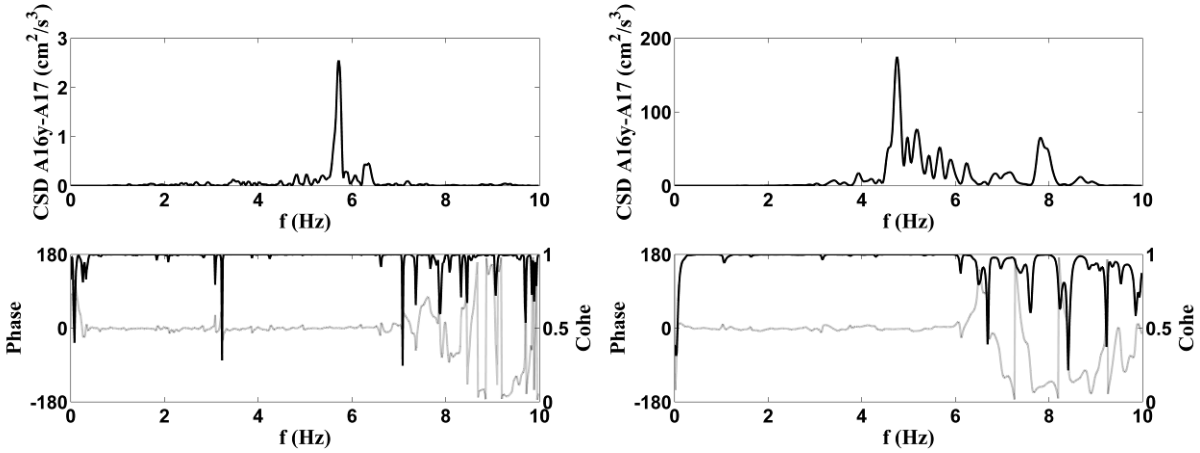

Fig. 11 – Cross spectral density in the 2013 earthquake: building B.

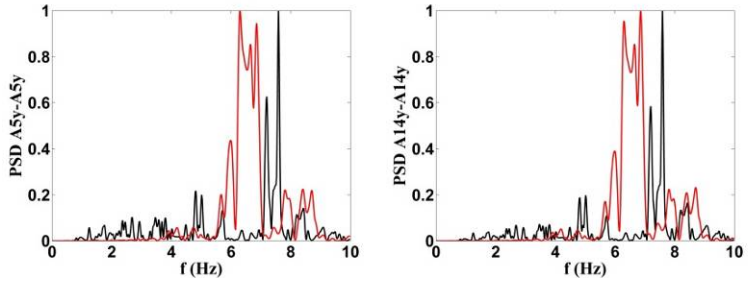

Fig. 12 – Normalized auto spectral density in the 2013 (black) and 2014 (red) earthquakes: building A.

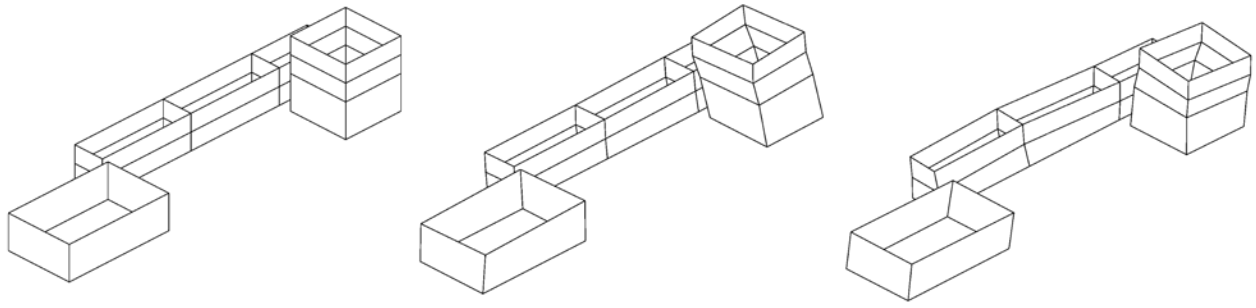

Fig. 13 – Undeformed and deformed shapes of the monitored buildings during the 2014 event: (a) undeformed; (b) opening of the structural joint between building T and A; (c) opening of the joint between building A end B .

The modal damping has been estimated by the well known method proposed in [8]. In particular, given that the singular values at frequency peaks are estimates of the auto spectral density associated with each mode, the inverse Fourier transform of each portion of the spectrum close to each peak gives the auto-correlation function of the modal single degree-of-freedom oscillator (Fig. 17). After observation of the local maxima in the function, the logarithmic decrement δ is evaluated by the following equation:

$$\delta = \frac{1}{j} \ln\left(\frac{u_1}{u_{j+1}}\right) \tag{1}$$

where u_j are the maxima in the correlation function. The damping ratio is given by:

$$\xi = \frac{\delta}{\sqrt{\delta^2 + 4\pi^2}} \tag{2}$$

Table 5 shows the damping ratio associated with the first four modal shapes, for the two considered earthquakes. Except for the second one, the damping is larger in the 2014 event, as expected.

Table 5 – Damping ratio

	x	
Mode	2013	2014
1	0.082	0.128
2	0.071	0.050
3	0.075	0.118
4	0.069	0.095

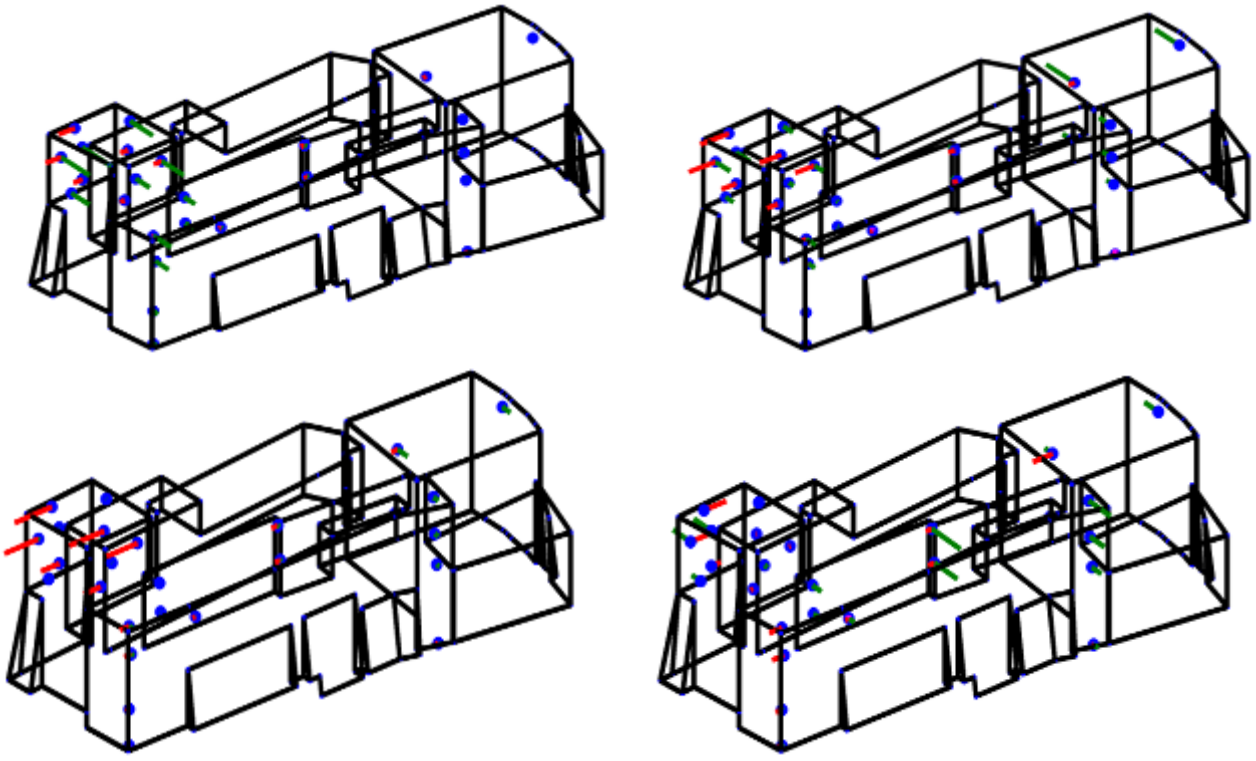

Fig. 14– First four modal shapes detected in the 2013 earthquake: sensor location (blue dot), X-component (red arrow), Y-component (green arrow).

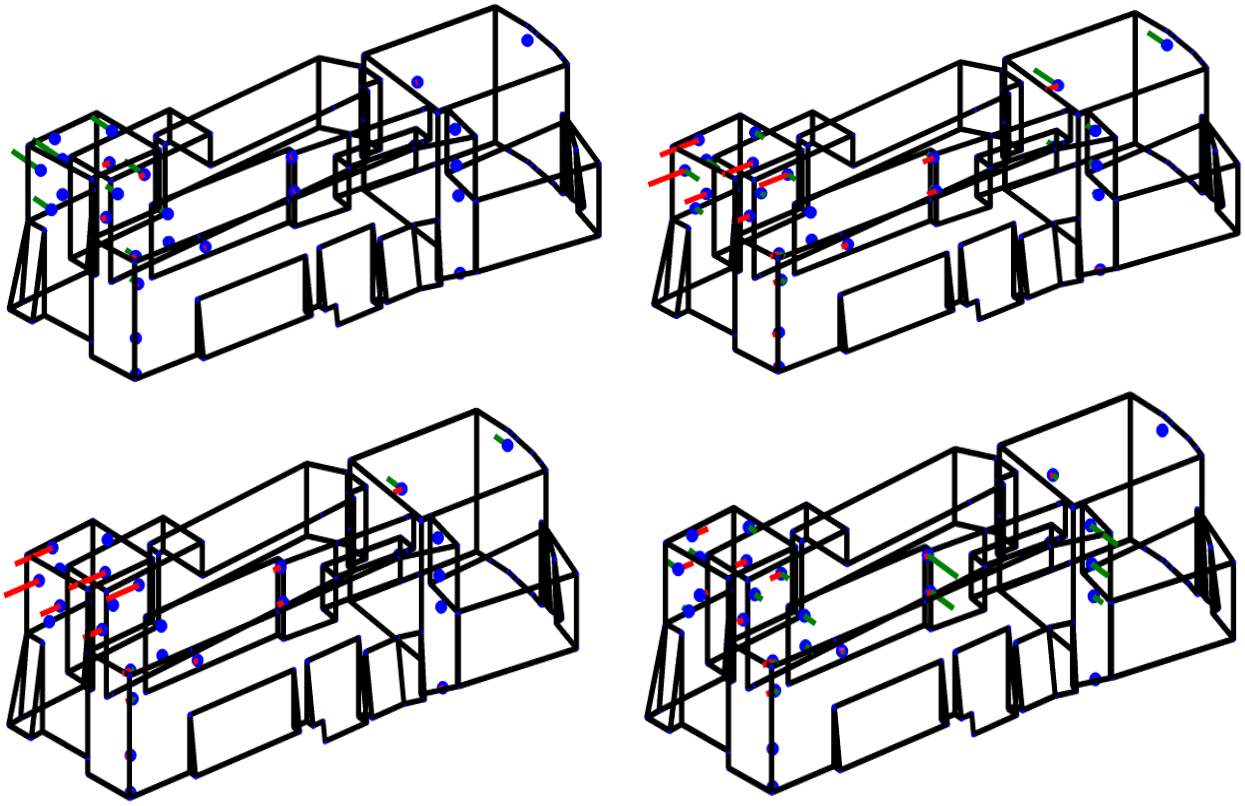

Fig. 15– First four modal shapes detected in the 2014 earthquake: sensor location (blue dot), X-component (red arrow), Y-component (green arrow).

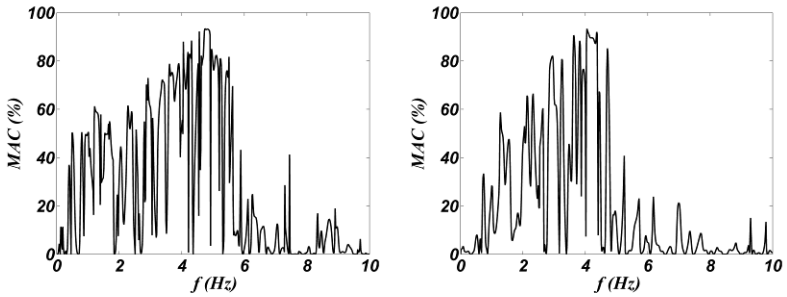

Fig. 16 – MAC value versus frequency for the first analytical mode, in the 2013 and 2014 earthquakes.

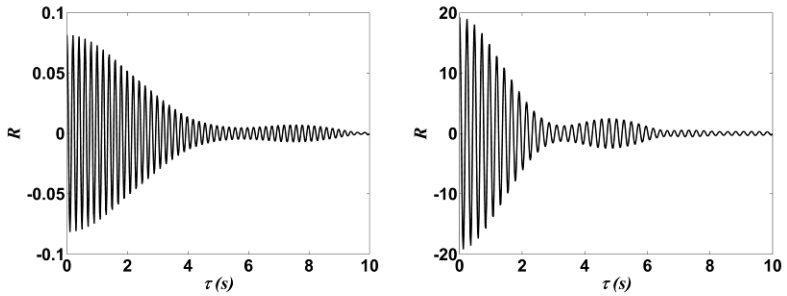

Fig. 17 – Auto correlation function associated with the first mode, in the 2013 and 2014 earthquakes.

6 Conclusions

The results gathered from the recordings of a seismic monitoring system installed on a historical building have been discussed. The ambient vibration analysis, performed using a temporary seismometers array, and a structural identification using a FEM model, allowed pointing out the dynamic characteristics of the structure. An average elastic modulus of the material equal to $E=2.3\cdot10^9 N/m^2$ has been found.

The analysis of the seismic events recorded on December 2013 and December 2014 highlighted significant shifts in the resonance frequencies. These were associated to modal shapes almost coincident. So the frequency reduction can be related to nonlinear behavior of masonry, which translates, with the increasing of the vibration amplitude, in a higher flexibility of the structure. This effect is present also in absence of damage; indeed, in the present case, the maximum recorded interstorey drift is far from the damage threshold.

Future development of this study should include the experimental analysis of the dynamic behavior of the building under stronger earthquakes, the experimental check of the dynamic characteristics after such earthquakes and a numerical modelling that includes the non-linear behavior of masonry. Finally the effectiveness of the joints should be investigated in detail.

Acknowledgements

The activities here described are part of a research project organized by ENEA in collaboration with the Italian National Civil Protection, the Office for the reconstruction of San Giuliano di Puglia after the 2002 earthquake and the Municipality of San Giuliano di Puglia.

References

[1] Bongiovanni G, Buffarini G, Clemente P, Rinaldis D, Saitta F, Nicoletti M, De Sortis A, Rossi G (2013): Dynamic Identification of Palazzo Marchesale in S. Giuliano di Puglia. In Zingoni A. (ed.) *Research and Applications in Structural Eng., Mechanics and Computation*: *Proceedings of the Fifth Int. Conf. on Structural Eng., Mechanics & Computation*, Taylor & Francis Group, London, 81-86, ISBN 978-1-136-00061-2.

[2] Buffarini G., Clemente P., Saitta F., Rossi G. (2014): Nonlinear analysis of an historical building under earthquake loading. *Proc. 10th U.S. National Conf. on Earth. Eng. (10NCEE)*, Earth. Eng. Research Institute, Anchorage, AK, 21-25 July, Paper 1012, DOI: 10.4231.D31G0HV72.

[3] Bendat JS, Piersol AG (1993): *Engineering applications of correlation and spectral analysis*. Wiley, 2nd edition.

[4] Brincker R, Zhang L, Andersen P (2000): Modal identification from ambient responses using Frequency Domain Decomposition. *18th Int. Modal Analysis Conference IMAC*, S. Antonio, Texas, USA.

[5] Dolce M, Nicoletti M, De Sortis A, Marchesini S, Spina D, Talanas F (2015): Osservatorio Sismico delle Strutture: the Italian structural seismic monitoring network. *Bulletin of Earthquake Engineering*, **13**(3).

[6] Gorini A, Nicoletti M, Marsan P, Bianconi R, de Nardis R, Filippi L, Marcucci S, Palma F, Zambonelli E (2010): The Italian strong motion network. *Bulletin of Earthquake Engineering*, 8:1075–1090.

[7] Zhang L, Brincker R, Andersen P (2001): Modal indicators for operational modal identification. *19th International Modal Analysis Conference IMAC*, Kissimmee, Florida, USA.

[8] Brincker R, Ventura CE, Andersen P (2001): Damping Estimation by Frequency Domain Decomposition. *Proceedings of IMAC 19: A Conference on Structural Dynamics*, Hyatt Orlando, USA.